ELSEVIER

Polymer 40 (1999) 1481–1485

polymer

Temperature dependence of dynamic yield stress in amorphous polymers as indicator for the dynamic glass transition at negative pressure

R. Lach[a], W. Grellmann[a], K. Schröter[b], E. Donth[b,*]

[a]*Fachbereich Werkstoffwissenschaften, Martin-Luther-Universität, Halle-Wittenberg, D-06099 Halle (Saale), Germany*
[b]*Fachbereich Physik, Martin-Luther-Universität Halle-Wittenberg, D-06099 Halle (Saale), Germany*

Received 22 January 1998; revised 9 April 1998; accepted 7 May 1998

Abstract

The dynamic yield stress for polycarbonate, polystyrene and poly(methyl methacrylate) was measured by an instrumented Charpy impact tester in a wide temperature range. The dynamic yield stress is interpreted as being proportional to a negative pressure. The temperature dependence can be described by a Williams–Landel–Ferry type of equation. The extrapolation to ambient pressure leads to the main α transition and is used to connect the dynamic yield stress to the pressure dependence of the α dispersion zone.

Keywords: Glass transition; Pressure dependence; Dynamic yield stress

1. Introduction

A well known property of the dynamic glass transition or α relaxation is the non-Arrhenius temperature dependence of the characteristic relaxation time, τ [1]. Its trace in an activation plot, $\log \tau$ as a function of $(1/T)$, is curved, especially for so-called fragile glass formers [2,3]. This dependence can be described by the Williams–Landel–Ferry (WLF) equation [4] for constant pressure, p

$$\ln\left[\frac{\Omega}{f(T,p)}\right]\left[T - T_\infty(p)\right] = \ln\left[\frac{\Omega}{f(T_0,p)}\right]\left[T_0 - T_\infty(p)\right] \qquad (1)$$

or analogously by a Vogel–Fulcher–Tamman–Hesse equation [5–7]. Here f is the frequency and T the temperature. The subscript 0 refers to an arbitrary reference point. T_∞ is the Vogel temperature and Ω is the high-frequency asymptote, which means the relaxation frequency formally extrapolated to $T \rightarrow \infty$ (for low-molecular-weight glasses, $\Omega = 10^{12}$–10^{15} Hz; for the glass transition of polymers, $\Omega \approx 10^{13}$ Hz [8]). Both asymptotic parameters may in principle be pressure-dependent, but we assume that Ω is practically not influenced by p.

Another characteristic property of the dynamic glass transition zone is the considerable width on logarithmic time or frequency scales corresponding to the non-exponential nature of the underlying time correlation functions: we have not only a single relaxation time τ, but rather a dispersion zone. There is growing evidence that this dispersion zone in high-molecular-weight polymers is composed of different contributions with even different temperature dependences [9–12].

The influence of hydrostatic pressure is rarely investigated in comparison to the vast amount of experimental work on the temperature dependence of τ. This is connected with the more complicated experimental problems in handling high pressures of up to several thousand bar. Mechanical and dielectric measurements [13–15] show a shift of the α relaxation zone to higher temperatures (lower frequencies) with increasing pressure. This can be understood by the free volume picture: increasing pressure diminishes the free volume. The location of secondary (β) relaxations, however, is approximately pressure-independent, because the β relaxation is not sensitive to free volume [16].

Investigations of the pressure dependence of the α relaxation time over wide pressure ranges [17] show a curvature analogous to the temperature dependence cited above. This can be parameterized in an equation equivalent to Eq. (1) [18], by exchanging pressure p for temperature T as another intensive thermodynamic quantity:

$$\ln\left[\frac{\Omega}{f(T,p)}\right]\left[p - p_\infty(T)\right] = \ln\left[\frac{\Omega}{f(T_0,p)}\right]\left[p_0 - p_\infty(T)\right] \qquad (2)$$

Here $p_\infty(T)$ is a lower limit pressure ('Vogel pressure').

* Corresponding author.

0032-3861/98/$ - see front matter
PII: S0032-3861(98)00365-6

Mathematically, $p_\infty(T)$ is the reverse function of $T_\infty(p)$. The comparison of Eqs. (1) and (2) for isochronous situations (frequency f = const.) yields [8]

$$p = \frac{C(f)}{T - \Theta} + \Pi \tag{3}$$

This equation has three parameters: the high temperature asymptote Θ, the pressure asymptote $\Pi < 0$ and $C(f)$. Both asymptotes can also be interpreted by means of the free volume picture: beyond Θ or Π — i.e., $T > \Theta$ or $p < \Pi < 0$ — there is always enough free volume so that there is no need for cooperative motion, independent of p or T, respectively. The parameter $C(f)$ increases with frequency and is a measure of the curvature for the isochrones in a p–T plot ('p–T fragility'). This curvature means that only moderate negative pressures are needed for generation of cooperative mobility, smaller than expected from a linear extrapolation of (dT_g/dp) near the glass transition temperature, T_g [8,18].

Measurements at large negative pressures would be especially interesting to get reliable values for the pressure asymptote Π. No techniques are known, however, to achieve negative hydrostatic pressures of the order of 100 MPa. But anelastic deformations of polymers in the glassy zone develop high local stresses that can be connected with negative pressures. The deformation velocity or reciprocal fracture time plays the role of a frequency for the dispersion zone.

In the instrumented Charpy impact test (see below), the sample is subjected mainly to a bending deformation as a multi-axis stress situation with a hydrostatic component. An analogous situation could be hydrostatic stress in the deformation zone in front of crazes [19,20]. For the formation of fibrils in crazes at low temperatures and high stresses, the α relaxation has been shown to be one of the mechanisms responsible [20,21]. This points to yielding as a cooperative phenomenon [22] which is not mainly connected to secondary relaxation processes [23].

In the following we restrict ourselves to bending stress experiments since they give a directly measured quantity that is, according to the von Mises and related criteria [24,25], an equivalence stress. This stress characterizes the special multi-axis stress situation. For other stress conditions other equivalence stresses would be necessary [26]. The estimated value of the asymptote Π_σ (see below) may vary for different stress situations [22].

The aim of this paper is to show that the yield stress behaves as a negative pressure according to Eq. (3), and that its temperature dependence leads to the dynamic glass transition zone at ambient pressure.

2. Experimental

2.1. Materials

The amorphous polymers investigated — polycarbonate (PC), polystyrene (PS) and poly(methyl methacrylate) (PMMA) — are commercial products with high molecular weight.

2.2. Instrumented Charpy impact test

An instrumented Charpy impact test was used for evaluation of the mechanical properties in the non-linear deformation range under dynamic load conditions. This is an alternative possibility to test the impact strength [27].

A significant improvement of the conventional Charpy impact test is achieved by instrumentation (Fig. 1) which combines a separate registration of the time dependence of the force F with the help of semiconductor strain gauges, and of the deflection v by an optoelectronic system. The dynamic yield stress, σ_{yd}, was derived from force–deflection diagrams (Fig. 2). The point in the stress–strain curve where the slope is zero for the first time, as the more technical definition of yield stress, is not used, because that point

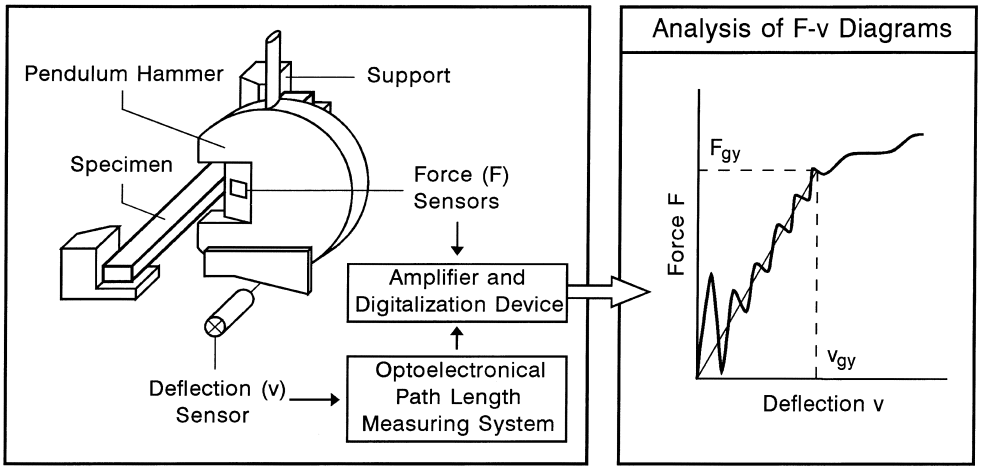

Fig. 1. Schematic construction of the Charpy impact tester and determination of the dynamic yield stress σ_{yd} from F_{gy} (by Eq. (4)), i.e., from the transition from elastic to elastic–plastic material behaviour.

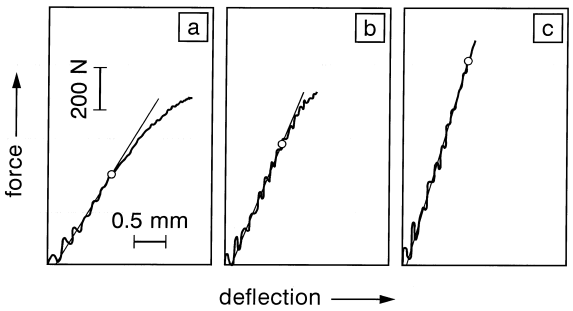

Fig. 2. Examples of force–deflection diagrams for (a) PC, (b) PS and (c) PMMA at room temperature. The symbol ○ indicates the change from elastic to elastic–plastic behaviour. The roughness of the curves is due to sample vibrations.

does not characterize the beginning of microscopic anelastic deformations. The technically defined variable has another temperature dependence [22,28] and a strong dependence on sample dimensions.

Our dynamic yield stress σ_{yd} is evaluated from the force, F_{gy}, at the transition from elastic to elastic–plastic material behaviour (points ○ in Fig. 2) by

$$\sigma_{yd} = F_{gy}\frac{3s}{2BW^2} \tag{4}$$

Three-point bending specimens with length $L = 2s = 80$ mm, width $W = 10$ mm and thickness $B = 4$ mm are used. The impact velocity was always $1.5\ \mathrm{m\ s^{-1}}$. This ensures a high deformation rate and minimizes the influence of relaxation processes on the shape of the force–deflection curve. The temperature range is from 80 K to 433 K.

A characteristic frequency of deformation (60–1100 Hz) was estimated as the fourth part of the inverse time to reach

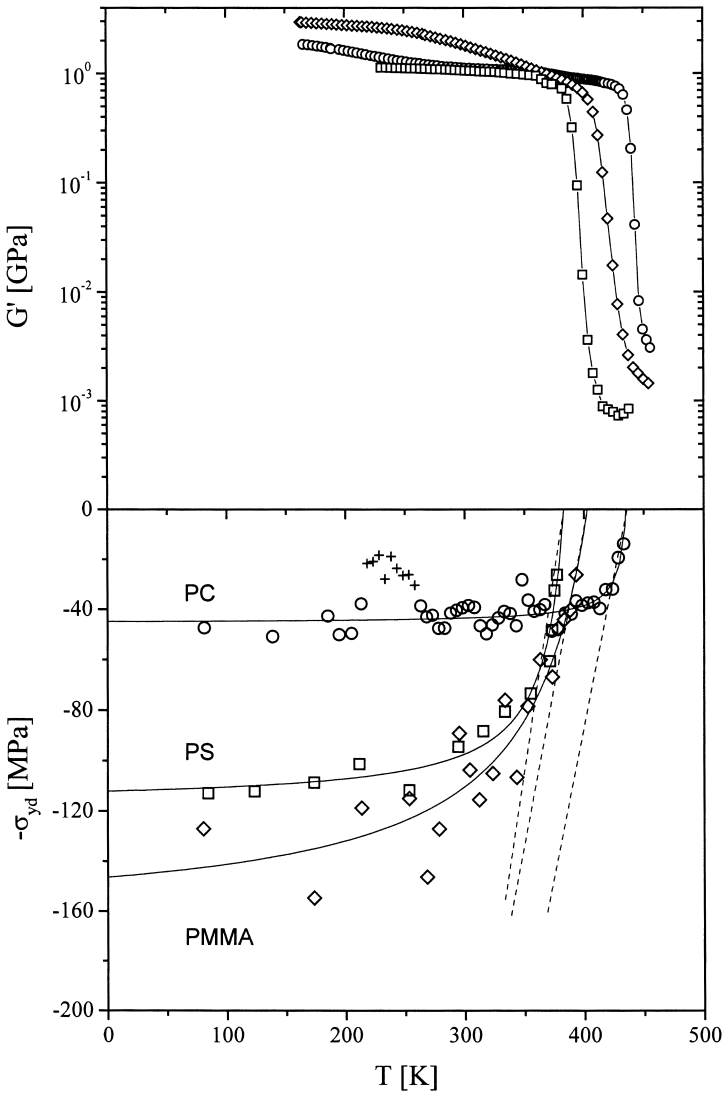

Fig. 3. Upper part: temperature dependence of the real part of shear modulus, G', for PC (○), PS (□) and PMMA (◇), corresponding to characteristic frequencies of the Charpy impact test. Lower part: dynamic yield stress, σ_{yd}, as a function of temperature. The curves are best fits to Eq. (3). The dashed straight lines are the slopes dp/dT_g at T_g from the literature [15,30–32].

the maximum force value in the time-resolved force–deflection measurement [29].

2.3. Dynamic mechanical analysis (d.m.a.)

The shear modulus in the linear deformation range was measured in the frequency range from 0.1 to 10 Hz with a Rheometrics RDA II analyser. This frequency range allows an extrapolation from d.m.a. measurements to the typical frequencies of the Charpy impact test.

3. Results

The lower part of Fig. 3 shows the dynamic yield stress, σ_{yd}, as a function of temperature for the three polymers. The stress is plotted on the negative ordinate to facilitate the comparison with negative pressures in Eq. (3). The scatter results mainly from the problem of fixing the value of F_{gy}. For instance, resonance vibrations of the sample disturb the curves in Fig. 2. This problem is sample-dependent.

The temperature dependence of the yield stress is described by a WLF-type equation (Eq. (3)) if the molecular mechanism responsible is related to the main transition. Fits with such functions (formally identifying $-p$ with σ_{yd}) are also shown in the lower part of Fig. 3. They reproduce the experimental values within experimental uncertainty. The hump for polycarbonate near $T \approx 220$ K is ascribed to the β relaxation and was not considered in the fit procedure [29]. The estimated temperature and stress asymptotes (Θ and Π_σ) and the values for the parameter C are collected in Table 1. Also included are the temperatures T_F obtained by an extrapolation to $\sigma_{yd} = 0$ corresponding to $p = 0$ in Eq. (3).

This temperature T_F corresponds to the onset of relevant microscopic deformations at low stresses ($\sigma_{yd} = 0$). The question of which kind of deformation occurs there can partly be decided by comparison with shear curves in the linear regime across the main transition for ambient pressure (upper part of Fig. 3, showing the real part of shear modulus, G', as function of temperature for the three different polymers).

To compare the G' curves with the results of the Charpy impact test, the frequency difference between the two devices must be taken into account. D.m.a. measurements at different frequencies were used to estimate shift factors [29]. In Fig. 3 the whole G' curves were shifted horizontally to the corresponding characteristic frequencies of the Charpy impact tests (see Table 1).

From the d.m.a. curves a temperature $T_{F,DMA}$ at the upper end of the main transition was estimated by a tangent construction for each sample. The values are also included in Table 1 for a comparison with the T_F values from the non-linear deformation of the Charpy impact test.

4. Discussion

The interpretation of dynamic yield stress σ_{yd} as a negative pressure $-p$ would rest on the supposition that we have an isotropic and homogeneous initial state. This cannot be expected for our experiments. Our evaluation for $p < 0$ by Eq. (3) remains correct, however, if both variables are proportional to each other and if the process responsible remains the same. The latter is supported by the correspondence between T_F and $T_{F,DMA}$ in Table 1.

To connect the $T_g(p)$ curves for $p > 0$ and $p < 0$ we would need only a proportionality between σ_{yd} and p. This is taken from the slope of the $T(\sigma_{yd})$ curves at $\sigma_{yd} = 0$ compared with the slopes of $T_g(p)$ curves from the literature. Both slope values are listed in Table 1.

A further problem is physical ageing. It is known [33,34] that the yield stress increases with ageing time. All samples were investigated in comparable ageing states so that no major influence on the shape of the curves in Fig. 3 is expected.

The concept of negative pressure is not intended to describe the solidification by orientation or to develop a fracture criterion. The latter would need fracture concepts and micromechanics [35,36].

Fig. 3 shows that the strong stress (or pressure) dependence of the glass transition temperature at low stresses cannot be extrapolated to large values of negative stresses. The curve is bent, and a stress asymptote Π_σ of the order of 100 MPa can be estimated. This value is much smaller than the linear extrapolation of dp/dT_g to very low temperatures,

Table 1
Values of stress and temperature asymptotes (Π_σ and Θ, respectively), and parameter C (Eq. (3)); values of temperatures T_F and $T_{F,DMA}$, the latter extrapolated from d.m.a. measurements to typical frequencies f of Charpy impact test; slopes of the measured stress dependence of T_g and values for the pressure dependence of T_g from literature; and negative pressure asymptote Π estimated from the slope scaling (see text)

Polymer	$-\Pi_\sigma$ (MPa)	$-C$ (MPa K)	Θ (K)	T_F (K)	$T_{F,DMA}$ (K)	f (Hz)	$dT_g/d\sigma_{yd}$ (K/100 MPa)	dT_g/dp (K/100 MPa)	$-\Pi$ (MPa)
PC	45.5 ± 1.5	297 ± 117	442 ± 5	436 ± 8	≈ 450	60	14 ± 7	42[a]	15 ± 8
PS	117 ± 5	1980 ± 680	400 ± 8	383 ± 15	≈ 408	620	14 ± 6	32[b]	53 ± 25
PMMA	165 ± 18	8450 ± 4360	454 ± 28	403 ± 60	≈ 437	1100	31 ± 23	40[c]	128 ± 109

[a]From [15].
[b]From [30,31].
[c]From [32].

indicated as dashed lines in Fig. 3. This finding supports the expected hyperbolic pressure dependence of the dynamic glass transition [8]. With the help of the proportionality between σ_{yd} and p, mentioned above, a true pressure asymptote Π can be estimated from Π_σ. This is also included in Table 1. The large errors result from the error in both Π_σ and the slope $d\sigma_{yd}/dT$ at low pressures. The Π values obtained correspond roughly to the values predicted from the curvature d^2T_g/dp^2 for $p > 0$ [37].

Scaling of responsible length scales across the dispersion zone is expected in the frame of a fine structure concept for the dynamic glass transition [12]. The length scale corresponding to hindered flow processes between the entanglement spacing (of the order of 5 nm) is expected at the low-frequency (or high-temperature) end of the α dispersion zone [38]. The temperature $T_{F,DMA}$ was therefore defined at this side of the modulus step. At present, the accuracy of the extrapolated values of T_F from the temperature dependence of the yield stress is too low for a definite assignment to special processes within the broad α dispersion zone.

Craze formation under tensile creep conditions in PC and styrene–acrylonitrile copolymer (SAN) in a certain temperature interval below T_g can also be connected with a continuation of both main ($T_g(p)$) and flow transition ($T_{FT}(p)$) to negative pressure [20]. It seems interesting that the pressure asymptote for the flow transition has a smaller value than for the main transition. This results in an intersection of $T_g(p)$ and $T_{FT}(p)$ curves.

5. Conclusions

The temperature dependence of the dynamic yield stress, σ_{yd}, for isochronous situations is described by the WLF-type equation (3). This supports the equivalence of this stress with a negative hydrostatic pressure. After scaling of $d\sigma_{yd}/dT_g$ with dT_g/dp at T_g, for our polymers the pressure asymptotes, Π, at low temperature are estimated to range from -15 to -130 MPa. Extrapolation of the $\sigma_{yd}(T)$ curves to low stresses gives a temperature near the dynamic glass transition zone as estimated for the relevant frequencies from linear response measurements. The anelastic deformation process is thus related to the dynamics of the main transition at negative pressure. Within experimental accuracy a definite assignment to components of the fine structure of the main transition was not possible. This needs further investigation.

Acknowledgements

Financial support by the Deutsche Forschungsgemeinschaft (DFG, Graduiertenkolleg ‘Polymerwissenschaften’) and the Fonds der Chemischen Industrie (FCI) is gratefully acknowledged.

References

[1] Ferry JD. Viscoelastic properties of polymers. New York: Wiley, 1980.
[2] Angell CA. In: Ngai KL, Wright GB, editors. Relaxations in complex systems. Washington, DC: Government Printing Office, 1985:1.
[3] Hodge IM. J Non-Cryst Solids 1996;202:164.
[4] Williams ML, Landel RF, Ferry JD. J Am Chem Soc 1955;77: 3701.
[5] Vogel H. Phys Z 1921;22:645.
[6] Fulcher GS. J Ceram Soc 1925;8:339.
[7] Tammann G, Hesse W Z Anorg Allg Chem 1926;156:245.
[8] Donth E, Conrad R. Acta Polym 1980;31:47.
[9] Donth E, Schneider K. Acta Polym 1985;36:213.
[10] Donth E, Schneider K. Acta Polym 1985;36:273.
[11] Ngai KL, Plazek DJ. J Rubber Chem Technol 1995;68:376.
[12] Donth E, Beiner M, Reissig S, Korus J, Garwe F, Vieweg S, Kahle S, Hempel E, Schröter K. Macromolecules 1996;29:6589.
[13] Williams G, Edwards DA. Trans Faraday Soc II 1966;62:1329.
[14] Schouten JA, Schotten J, Nelissen L, Nies E. Polym Commun 1991;32:421.
[15] Zoller P. J Polym Sci, Polym Phys Edn 1982;20:1453.
[16] Quinson R, Perez J, Germain Y, Murraciole JM. Polymer 1995;36:743.
[17] Paluch M, Ziolo J, Rzoska SJ, Habdas P. J Phys: Condens Matter 1997;9:5485.
[18] Donth E. Relaxation and thermodynamics in polymers. Glass transition. Berlin: Akademie Verlag, 1992.
[19] Donth E, Michler G. Colloid Polym Sci 1989;267:557.
[20] Starke J-U, Schulze G, Michler GH. Acta Polym 1997;48:92.
[21] Starke J. Thesis. Halle-Wittenberg: Martin-Luther-Universität, 1997.
[22] Chow TS. Polym Eng Sci 1996;36:2939.
[23] Watts DC, Perry EP. Polymer 1978;19:248.
[24] Kinloch AJ, Young RY. Fracture behaviour of polymers. London/ New York: Elsevier Applied Science Publishers, 1985.
[25] Ehrenstein GW. Polymer-Werkstoffe. München/Wien: Carl Hanser, 1978.
[26] Haward RN, Murphy BM, White E. J Polym Sci Part A2 1971;9:801.
[27] Grellmann W, Seidler S, Hesse W. Ermittlung des Rißwiderstandsverhaltens aus dem instrumentierten Kerbschlagbiegeversuch. In: Grellmann W, Seidler S, editors. Deformation und Bruchverhalten von Kunststoffen. Berlin/Heidelberg: Springer, 1998.
[28] Bauwens JC. J Mater Sci 1972;7:577.
[29] Lach R. Korrelationen zwischen bruchmechanischen Werkstoffkenngrößen und molekularen Relaxationsprozessen amorpher Polymere, Fortschritt-Berichte, Reihe 18: Mechanik/Bruchmechanik. Düsseldorf: VDI-Verlag, 1998.
[30] Quach A, Simha R. J Appl Phys 1971;42:4592.
[31] Takamizawa K, Toratani H, Karasz FE. Thermoch Acta 1994;240: 23.
[32] Schneider HA. J Therm Anal 1996;47:453.
[33] Struik LCE. Physical aging in amorphous polymers and other materials. Amsterdam: Elsevier, 1977.
[34] Bauwens-Crowet C, Bauwens JC. Polymer 1982;23:1599.
[35] Grellmann W, Lach R. Angew Makromol Chem 1996;237:191.
[36] Grellmann W, Che M. J Appl Polym Sci 1997;66:1237.
[37] Donth E. Glasübergang. Berlin: Akademie, 1981.
[38] Vieweg S, Unger R, Hempel E, Donth E. J Non-Cryst Solids, in press.